THE ROYAL SOCIETY

Adherence and drug resistance: predictions for therapy outcome

Lindi M. Wahl and Martin A. Nowak

Institute for Advanced Study, Olden Lane, Princeton, NJ 08540, USA

We combine standard pharmacokinetics with an established model of viral replication to predict the outcome of therapy as a function of adherence to the drug regimen. We consider two types of treatment failure: failure to eliminate the wild-type virus, and the emergence of drug-resistant virus. Specifically, we determine the conditions under which resistance dominates as a result of imperfect adherence. We derive this result for both single- and triple-drug therapies, with attention to conditions which favour the emergence of viral strains that are resistant to one or more drugs in a cocktail. Our analysis provides quantitative estimates of the degree of adherence necessary to prevent resistance. We derive results specific to the treatment of human immunodeficiency virus infection, but emphasize that our method is applicable to a range of viral or other infections treated by chemotherapy.

Keywords: adherence; resistance; HIV; immunology; virology; pharmacokinetics

1. INTRODUCTION

Imperfect adherence to a prescribed regimen is one of the critical obstacles to successful drug therapy. Maintaining adherence may be particularly difficult when the drug regimen is complex or side-effects are severe, as is often the case for current human immunodeficiency virus (HIV) therapy (Besch 1995; Ickovics & Meisler 1997; Katzenstein 1997; Mehta *et al.* 1997).

It is widely acknowledged that lack of adherence facilitates the emergence of drug resistance, but the precise mechanisms and conditions under which this occurs have not been elucidated (for a review, see Levin *et al.* 1998; Levin & Andreason 1999). The epidemiology of drug resistance has been well characterized (Austin *et al.* 1997; Bonhoeffer *et al.* 1997*a*; Davies 1997; Levin *et al.* 1997; Levy 1997; Austin *et al.* 1999; Levin & Andreason 1999), as has the emergence of drug resistance within an individual (Nowak *et al.* 1991, 1997; McLean & Nowak 1992; Frost & McLean 1994; Coffin 1995; Bonhoeffer & Nowak 1997; Lipsitch & Levin 1997; Stilianakis *et al.* 1997; Austin & Anderson 1999). Three recent papers have modelled the interaction of changing drug concentrations with the population dynamics of a pathogen (Austin *et al.* 1998; Kepler & Perelson 1998; Lipsitch & Levin 1998), examining in detail the conditions necessary for treatment success (Austin *et al.* 1998) or for the emergence of drug resistance (Kepler & Perelson 1998; Lipsitch & Levin 1998).

The US Department of Health and Human Services (1999) recently declared that 'clarification of the degree of adherence [to HIV therapy]... necessary to prevent resistance is urgently needed'. This question has begun to be addressed clinically, and sharp increases in virological failure rates have been correlated with decreasing adherence in prospective studies (Paterson *et al.* 1999). We examine this question theoretically, predicting treatment outcome as a function of adherence to a given drug regimen.

*Author for correspondence (wahl@ias.edu).

2. DOSE AND EFFECT

Although interpatient variation may be a significant factor, the average pharmacokinetic parameters of drugs used in HIV therapy are well established in humans. For any given drug, the recommended dosing interval T, the maximum concentration in plasma $C_{\max}$, and the serum half-life $T_{1/2}$ may be used to predict the time-course of the drug concentration in plasma, $C(t)$. For a more accurate model, the time to peak t_{p} may also be included. We use these parameters to build a simple model of the plasma time-course of the pharmaceutical, assuming a linear rise in drug concentration from the start of the dosing interval to t_{p}, and a single exponential decay thereafter:

$$C(t) = \begin{cases} C(T) + \frac{t}{t_{\mathrm{p}}}\left(C_{\max} - C(T)\right) & \text{for } 0 \leqslant t < t_{\mathrm{p}}, \\ C_{\max} \mathrm{e}^{-w(t-t_{\mathrm{p}})} & \text{for } t_{\mathrm{p}} \leqslant t \leqslant T, \end{cases} \tag{1}$$

where $w = \log(2)/T_{1/2}$. Note that $C_{\max}$ must be the maximum concentration achieved in plasma after a number of successive doses, such that the patient is in a 'steady state' with respect to any gradual accumulation of the drug.

This model provides an independent estimate of the trough concentration $C(T)$, and the area under the plasma concentration curve AUC, which can be compared to the known pharmacokinetic parameters as a verification of the model. A sample plasma time-course for a protease inhibitor is illustrated in figure 1. In this example a new dose of the drug is taken every 8 h and no doses are missed (perfect adherence).

To model imperfect adherence, we let p denote the fraction of the prescribed doses of the drug which are taken. If the drug is taken in a given dosing interval, equation (1) describes the time-course of drug concentration for that interval. If the drug is not taken, the dose decays from its current concentration with half-life $T_{1/2}$.

Received 4 January 2000 *Accepted* 11 January 2000

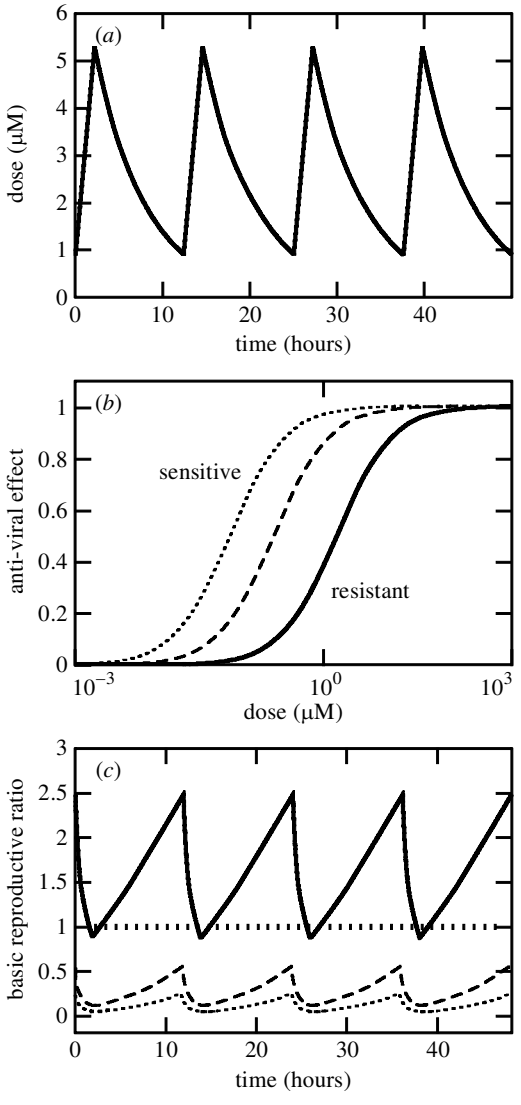

Figure 1. Plasma concentration time-course, dose effect curve, and the effect on the basic reproductive ratio. (*a*) The time-course of drug concentration in plasma. For this example we simulate the time-course of nelfinavir, with $T_{1/2} = 4$ h, $\mathcal{T} = 8$ h, $C_{\max} = 5.27\,\mu$M, $t_p = 2$ h and $p = 1.0$. (*b*) Dose effect curves for the drug-sensitive and drug-resistant viral strains. The IC_{50} for the drug-sensitive virus (dotted line) is $0.03\,\mu$M; for the resistant strains the IC_{50} is five times (dashed line) or 50 times (solid line) greater (0.15 or $1.5\,\mu$M, respectively). (*c*) The time-course of the basic reproductive ratio affected by the concentration time-course shown in panel (*a*). Here $R_0 = s\beta\lambda/da$, with $\lambda = 100$, $d = 0.1$, $a = 0.5$, and where s is the fractional antiviral effect illustrated in panel (*b*). For the drug-sensitive virus (dotted line), $\beta = 0.004$. For the drug-resistant virus (dashed and solid lines), $\beta = 0.002$. Note that the drug maintains R_0 close to zero for the drug-sensitive and partially resistant virus, but that R_0 for the 50-fold drug-resistant virus is greater than unity. In this example missing a single dose would allow R_0 of the fivefold resistant virus to exceed unity for several hours.

The level of adherence p reflects the long-term average of the number of doses taken. Adherence patterns may vary between individuals, commonly including total breaks in drug therapy (drug holidays) over a number of days. While the long-term mean adherence is a good prognostic for the long-term outcome of this dynamical system, we note that different patterns of adherence, even with the same value of p, may shift the balance in favour of the resistant or wild-type virus. We will return to this issue in the subsequent section.

Unless noted otherwise, we use the same pattern of adherence in each of the simulated examples that follow: the probability of taking a dose at the beginning of each interval is independent of previous history and is constant. Thus, for each new dosing interval the drug is taken with a probability equal to the long-term average adherence p. In this simple Poisson model we do not allow for drugs to be taken at time-points in between the dosing intervals.

Although the concentration of the pharmaceutical in plasma can be described with some accuracy, it is difficult to predict the time-course of intracellular concentrations of the drug. While the kinetics of drug entry to the intracellular space (for example to cells in lymph tissue), are almost certainly slower than the uptake in plasma, the egress or metabolism of the drug from the cytoplasm is largely unknown. Nonetheless, we can use the plasma concentration as a rough estimate of the time-course of the drug in the system. By neglecting dispersion and delay as the drug enters the intracellular space, we clearly overestimate the temporal effects of dosing at intervals, and therefore we hope to deduce conservative estimates of the need for adherence. (For a fuller treatment of the effects of spatially distinct compartments, see Kepler & Perelson (1998); for a detailed model of the kinetics of drug action, see Austin *et al.* (1998).)

Given this simple model of the time-course of drug concentration and an estimate of the dose–response profile for the drug, we can predict the time-course of the antiviral effect. Here we assume that the inhibition of viral replication s can be described by

$$s(t) = 1 - \frac{C(t)}{C(t) + \mathrm{IC}_{50}}, \qquad (2)$$

where IC_{50} is the concentration of drug which inhibits viral replication by 50%. Thus when $s \approx 1$ the drug has no effect, while if $s \approx 0$ the drug completely inhibits viral replication. Although the relationship between *in vitro* susceptibility of HIV to antiviral drugs and the *in vivo* inhibition of viral replication in humans has not been rigorously established, we use the *in vitro* IC_{50} value for each drug to provide an estimate of the *in vivo* value of s.

For a number of antiviral drugs, the increase in IC_{50} after the emergence of drug resistance in a viral population has been accurately quantified. These altered values of IC_{50} can therefore be used in equation (2) to compute s for drug-resistant strains. Examples of the dose–response curves predicted for the protease inhibitor nelfinavir, are shown in figure 1. HIV isolates from some patients treated with this drug have shown reduced susceptibility (fivefold to 93-fold) to nelfinavir *in vitro*, correlated with one or more mutations in the virus protease gene (for reviews, see Moyle & Gazzard 1996; Hoetelmans *et al.* 1997; McDonald & Kuritzkes 1997; Jarvis & Faulds 1998).

Figure 1*b* plots the dose–response curve for drug-sensitive virus (dotted line, $IC_{50} = 0.03\,\mu$M), partially resistant virus (dashed line, fivefold resistance), and highly resistant virus (solid line, 50-fold resistance).

Figure 1*c* illustrates the effect of s on the basic reproductive ratio of the virus R_0 over time. R_0, originally described in the ecology and epidemiology literature (Macdonald 1952; Dietz 1975, 1976; Yorke *et al*. 1979; May & Anderson 1979; Anderson & May 1991), is defined as the average number of secondary infected cells arising from one infected cell placed into an entirely susceptible cell population. In this example we see that the basic reproductive ratio of the drug-sensitive virus is held very close to zero, while R_0 for the fivefold drug-resistant strain (dashed line) is larger but still less than unity at all times. It is clear that, in this example, fivefold drug resistance implies that a single missed dose would allow R_0 to exceed unity for a number of hours. A 50-fold increase in resistance (solid line) allows the basic reproductive ratio of the virus to exceed unity almost continually.

3. VIRUS DYNAMICS

We use a simple model of virus dynamics (McLean & Nowak 1992; Bonhoeffer & Nowak 1997), in which we distinguish between susceptible cells x, cells infected with drug-sensitive virus y_1, and cells infected with drug-resistant virus, y_2. Let us assume that the susceptible cells are produced at a constant rate λ from a pool of precursor cells, and die at rate dx. Susceptible cells become infected at rates $s_1\beta_1 xy_1$ and $s_2\beta_2 xy_2$ by sensitive and resistant virus respectively, where β_1 and β_2 reflect the infectivity of sensitive and resistant virus strains. We assume that $\beta_1 > \beta_2$, that is, the wild-type virus is the most infectious strain in the absence of the drug.

Drug treatment is reflected in the parameters $s_1(t)$ and $s_2(t)$ (between zero and unity), which describe the inhibition of viral infectivity for the sensitive and resistant virus. The degree of inhibition is a function of the drug concentration at each time (equation (2)). Infected cells of both strains die with rate constant a. This yields the following system of ordinary differential equations:

$$\dot{x} = \lambda - dx - (s_1\beta_1 y_1 + s_2\beta_2 y_2)x, \tag{3}$$

$$\dot{y}_1 = (s_1\beta_1 x - a)y_1, \tag{4}$$

$$\dot{y}_2 = (s_2\beta_2 x - a)y_2. \tag{5}$$

This model has some documented shortcomings (McLean & Nowak 1992; Bonhoeffer & Nowak 1997*a*,*b*), which the inclusion of further parameters (such as the immune response) may serve to alleviate. We have limited our treatment in this paper to the basic model, but note that results might differ, at least quantitatively, if the immune response were included explicitly.

We use the model of $C(t)$ described above, for a given degree of adherence p, to compute both s_1 and s_2 as described in equation (2) and illustrated in figure 1. To model the effects of several drugs administered simultaneously, we compute the concentration time-course for each drug and then multiply the value of s computed for each drug to give the total inhibition at each time-point.

The differential equations described above can be simulated for a given drug regimen and adherence p. Figure 2 shows four examples of the progression of HIV over 18 months, for the same initial conditions but different degrees or patterns of adherence. Panels on the left plot virus load (number of infected cells) for the sensitive (solid line) and resistant (dotted line) viral strains; panels on the right show the drug concentration for the first ten days of treatment, which begins at day 30. We see that when $p = 1$ (figure 2*a*), the virus is rapidly eliminated from the body, while when $p = 0.3$ (figure 2*d*), treatment fails and the wild-type virus persists. For intermediate values of p (figure 2*b*,*c*), however, the outcome depends on the adherence pattern. For the Poisson model of adherence, the sensitive virus is eliminated but the drug-resistant virus persists. If dose-taking is slightly more 'clumped' than in the Poisson model however, the wild-type virus continues to dominate the population. We will discuss this result further in § 4.

Several interesting observations can be made at this point. Comparing perfect adherence with the Poisson example when $p = 0.5$, we note in both cases that immediately after the start of treatment the frequency of the drug-sensitive virus decreases. Because the initial frequency of the drug-resistant mutant is so small (in these examples 1 in 10^7), and because the basic reproductive ratio of the drug-sensitive virus is reduced by therapy to be just below that of the drug-resistant strain, there is a lag of more than eight months before the resistant strain begins to dominate the system. Thus, in the first few months of therapy, the situation when drug levels are adequate to eliminate the virus may be indistinguishable from the situation where an infectious drug-resistant mutant is growing exponentially from a tiny initial frequency, in competition with the wild-type virus, and only gradually dominating the system. Once the drug-resistant mutant has arisen, we note further that the total virus load may be nearly indistinguishable from the pre-treatment virus load (Bonhoeffer & Nowak (1997), but see § 5).

4. LONG-TERM OUTCOME OF THERAPY

(a) *Single-drug therapy*

We can analytically predict the outcome of therapy for a known adherence, p, and a simple adherence pattern. To do this, we first consider the variation in s over time, as depicted in figure 1. Because the variation in s is over a time-scale of hours, whereas the ultimate outcome of therapy occurs over the course of months or years, we are interested in the mean value of s, $\bar{s}(p)$, when adherence is p. As an example, equation (A3) (derived in Appendix A) approximates the value of $\bar{s}_1(p)$ and $\bar{s}_2(p)$ for the drug-sensitive and drug-resistant viral strains, respectively, using a Poisson model of adherence.

Using these results, we compute the mean value of the basic reproductive ratio for both the drug-sensitive virus (R_1) and drug-resistant virus (R_2):

$$\left.\begin{aligned}\bar{R}_1(p) &= \bar{s}_1\beta_1\lambda/da\\ \bar{R}_2(p) &= \bar{s}_2\beta_2\lambda/da\end{aligned}\right\}. \tag{6}$$

The mean values of these reproductive ratios serve as useful predictors of the long-term outcome of the system under several conditions: (i) the chance extinction of the drug-resistant strain is unlikely (true for HIV); (ii) the time-scale of consistent dose taking or doses

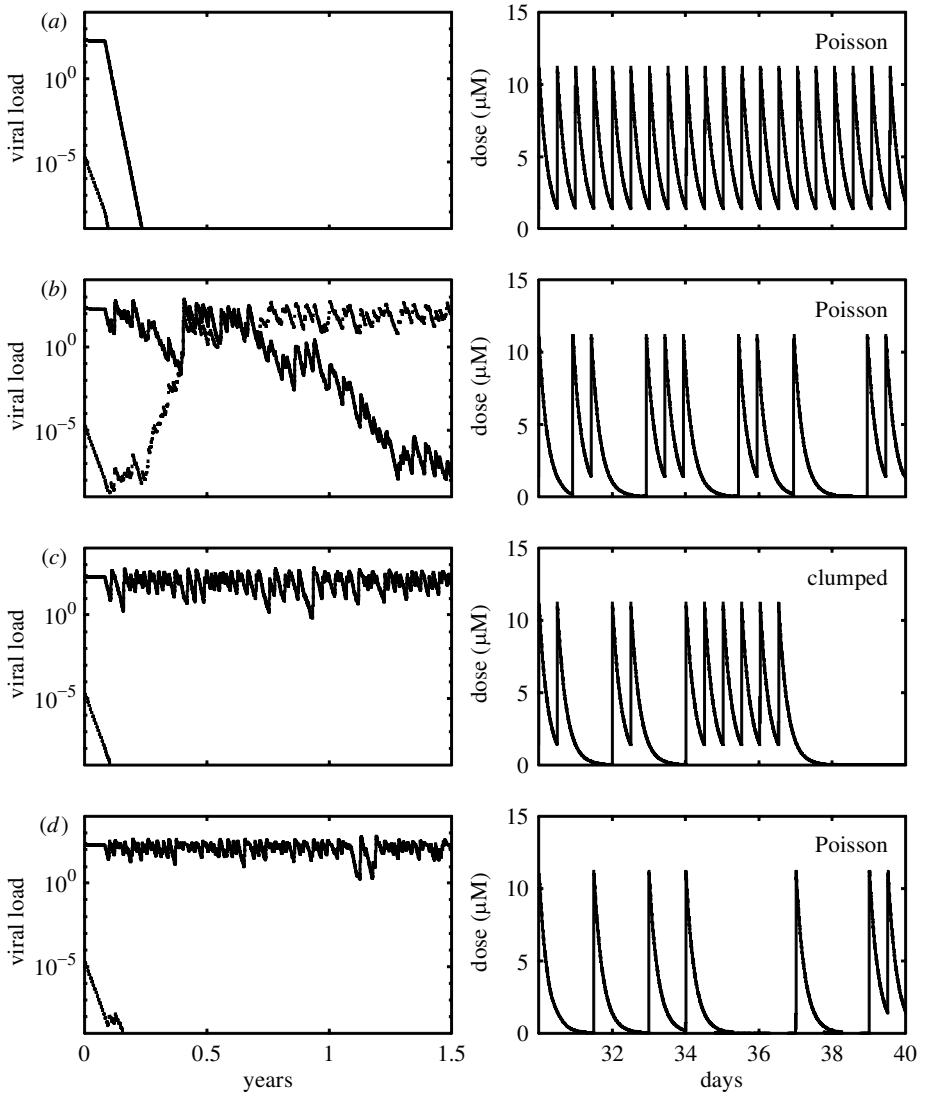

Figure 2. Simulated time-course of infection for four degrees and patterns of adherence. For this example we simulate the time-course of the protease inhibitor ritonavir, with $T_{1/2} = 4$ h, $T = 12$ h, $C_{max} = 11.2\,\mu g\,ml^{-1}$ and $IC_{50} = 0.0159\,\mu g\,ml^{-1}$. We assume that 1 in 10^7 infected cells are initially infected with a mutant strain of the virus and that these mutations confer a tenfold resistance to ritonavir. The level of adherence to the drug regimen was varied: $p = 1.0$ (*a*) $p = 0.5$ (*b*,*c*), and $p = 0.3$ (*d*). Panels on the left illustrate the total number of cells infected by drug-sensitive (y_1, solid line) and drug-resistant (y_2, dotted line) over 18 months. Panels on the right show the time-course of the drug concentration for the first ten days of treatment (note the change in time-scale) which begins at day 30. We find that with intermediate levels of adherence in a Poisson pattern, the drug-resistant strain dominates; this occurs only after some eight months of therapy, and fixation requires over 18 months. In (*c*) we provide an example with the same mean adherence, 0.5, but a 'clumped' pattern of dose-taking: every time a dose is taken, two doses are taken, and every time a dose is missed, two doses are missed. This simplistic model illustrates that the specific dose-taking pattern may change therapy outcome; treatment fails in this example. Simulations were performed by integrating equations (3)–(5) numerically with initial conditions $x(0) = 1000$, $y_1(0) = 500$ and $y_2(0) = 5 \times 10^{-5}$; other parameter values were $\lambda = 100$, $d = 0.1$, $a = 0.5$, $\beta_1 = 0.008$ and $\beta_2 = 0.004$.

missed is short compared to the characteristic times in equations (3)–(5) (thus the question of drug holidays cannot be addressed by our methods at present); and (iii) the variations in R_1 and R_2 are relatively smooth (this is true, for example, when doses decay smoothly and the dose–response curve is described by equation (2)). We note, however, that the long-term average of R_1 and R_2 are not simple functions of p, but also depend on the pattern of dose taking; we address this in figure 3*b*, described below.

For any adherence pattern, we know that $\beta_1 > \beta_2$, and so it is clear that when $p = 0$ (pre-treatment), $R_1(0) > R_2(0)$. Both R_1 and R_2 will be decreasing functions of p, but R_1 should fall faster as p increases. Thus, we expect that at some threshold value of adherence, the basic reproductive ratio of the drug-resistant virus will be larger than that of the drug-sensitive virus. If R_2 is greater than unity at this point, then the drug-resistant virus will experience exponential growth. This result is illustrated in figure 3*a*, which illustrates both R_1 and R_2 for p between zero and unity. For this example we study a Poisson model of adherence with the protease inhibitor indinavir, which is taken every 8 h and has a 2 h half-life. Phenotypic and genotypic testing of HIV isolates from patients treated with indinavir have shown three or four mutations in the virus protease gene which confer a

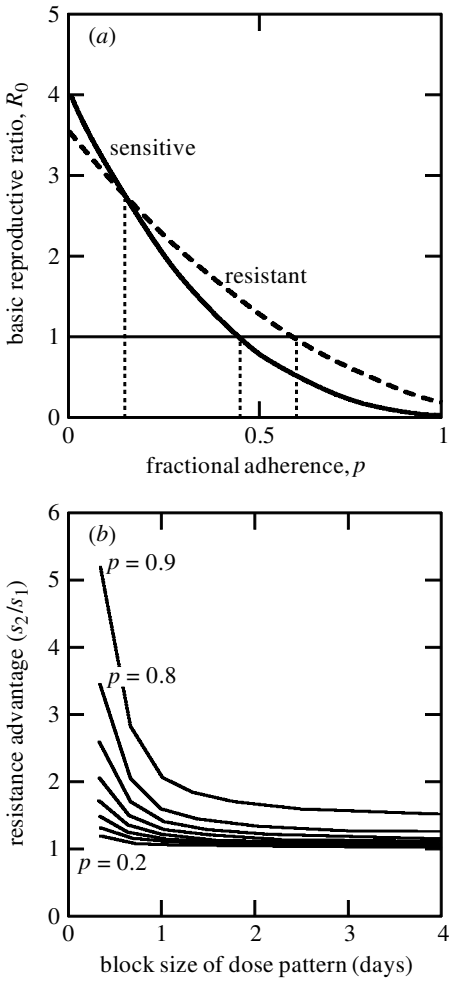

Figure 3. Basic reproductive ratio, adherence and adherence patterns. In (*a*), we determine R_1 and R_2 as described in equation (6), for $\beta_1 = 0.002$, $\beta_2 = 0.00175$, $\lambda = 100$, $d = 0.1$, $a = 0.5$. The values of $\bar{s}(p)$ are determined as described in equation (A3). In this example we use the Poisson adherence pattern and parameters which approximate the effect of the protease inhibitor indinavir ($T_{1/2} = 2$ h, $T = 8$ h and $C_{max} = 12.6\,\mu$M). For the drug-sensitive strain we set $IC_{50} = 5.3 \times 10^{-3}\,\mu$M, while IC_{50} for the drug-resistant strain is ten times greater (0.053 μM). For zero adherence (pre-treatment), $R_1 > R_2$, and the resistant strain will be out-competed. Note that for $p < 0.45$, treatment will fail to eradicate the virus even if the drug-resistant mutant does not exist ($R_1 > 1$). For $p > 0.6$, this model predicts treatment success. For adherence between 0.15 and 0.6, if the resistant mutant exists it will dominate the system. In (*b*) we use the same parameter values, but doses are taken or missed in blocks of n successive doses, between 8 h and 4 days or 1–24 doses. Here we illustrate the decreasing advantage of resistance ($\bar{s}_2/\bar{s}_1$) with increasing block size, for mean adherence (p) values between 0.2 and 0.9.

four- to eightfold resistance to the drug *in vitro* (for reviews, see Moyle & Gazzard 1996; Hoetelmans *et al.* 1997; McDonald & Kuritzkes 1997).

From figure 3, we see three separate regions of treatment outcome. When $p < 0.15$, the drug-sensitive virus dominates; treatment fails to eliminate the wild-type virus. For $0.15 < p < 0.6$, R_2 is larger than R_1, and R_2 is also larger than unity. In this large region treatment also fails, but it fails because of the emergence of the drug-resistant viral strain. Treatment succeeds in eliminating both strains of the virus when $p > 0.6$. We note further that there are two situations in which resistance dominates. For $0.15 < p < 0.45$, treatment is insufficient to eradicate either viral strain (both R_1 and R_2 are greater than unity), but resistance dominates because the drug suppresses the wild-type virus such that $R_2 > R_1$. In this region treatment would fail even if the drug-resistant mutant did not exist. If the drug-resistant mutant exists, however, it competes with the wild-type virus. The drug-resistant mutant may emerge as the dominant viral strain only gradually in this case, because the difference between R_2 and R_1 is not large (see, for example, figure 2, when $p = 0.3$). In contrast, for $0.45 < p < 0.6$, treatment would be sufficient to eradicate the wild-type virus if the drug-resistant mutant did not exist, and if the drug-resistant mutant does exist it will dominate the system rapidly.

In figure 3*b*, we explore the effect of different dose-taking patterns. As described in Appendix A, we can determine analytically the long-term average of the antiviral effect, $\bar{s}_1$ or $\bar{s}_2$, for a specified pattern of adherence. We define the resistance advantage as the ratio of these quantities, $\bar{s}_2/\bar{s}_1$. It is clear that for the resistant mutant to out-compete the wild-type, this resistance advantage must exceed the pre-treatment ratio of R_1/R_2. We computed the resistance advantage for a pattern of increasingly lengthy dosing 'blocks' of n successive doses or missed doses. Every nth dose, Poisson statistics identical to the Poisson model described above are used to determine whether doses will be taken for the following block of time: if a dose is taken, then n doses are taken successively; if a dose is missed, then n doses are missed successively. Thus doses are increasingly 'clumped' as the block size increases, while the long-term average adherence p is constant (the same fraction of total doses is taken irrespective of block size).

As illustrated in figure 3, doses which occur in blocks can reduce the advantage of resistance. Intuitively, we argue that resistance thrives under intermediate drug concentrations—high levels of the pharmaceutical reduce viral replication, while low levels do not sufficiently hinder the wild-type. Thus constraining doses to occur consecutively significantly decreases the amount of time during which drug concentrations are intermediate and the resistant virus has a replication advantage. This explains the failure to out-compete the wild-type strain illustrated for the 'clumped' dosing regimen in figure 2. The derivation of $\bar{s}_1$ and $\bar{s}_2$ for blocks of consistent dosing is provided in Appendix A.

In figure 3*a*, we set the pre-treatment $R_1(0) = 4$ and $R_2(0) = 3.5$. We generalize this result for different values of the basic reproductive ratios in figure 4. Here each panel shows the regions of treatment failure (hatching and shading) or treatment success (solid white). These regions are plotted for $R_1(0)$ between unity and ten on the y-axis. Each panel shows the result for $R_2(0)$ as a different (but constant) fraction of $R_1(0)$. The thick black line in each panel shows where R_1 drops below unity. Thus treatment failure will occur in the region to the left of this line (horizontal hatching), regardless of whether the resistant mutant exists. If the resistant mutant exists, it will dominate the system for parameter values shown in

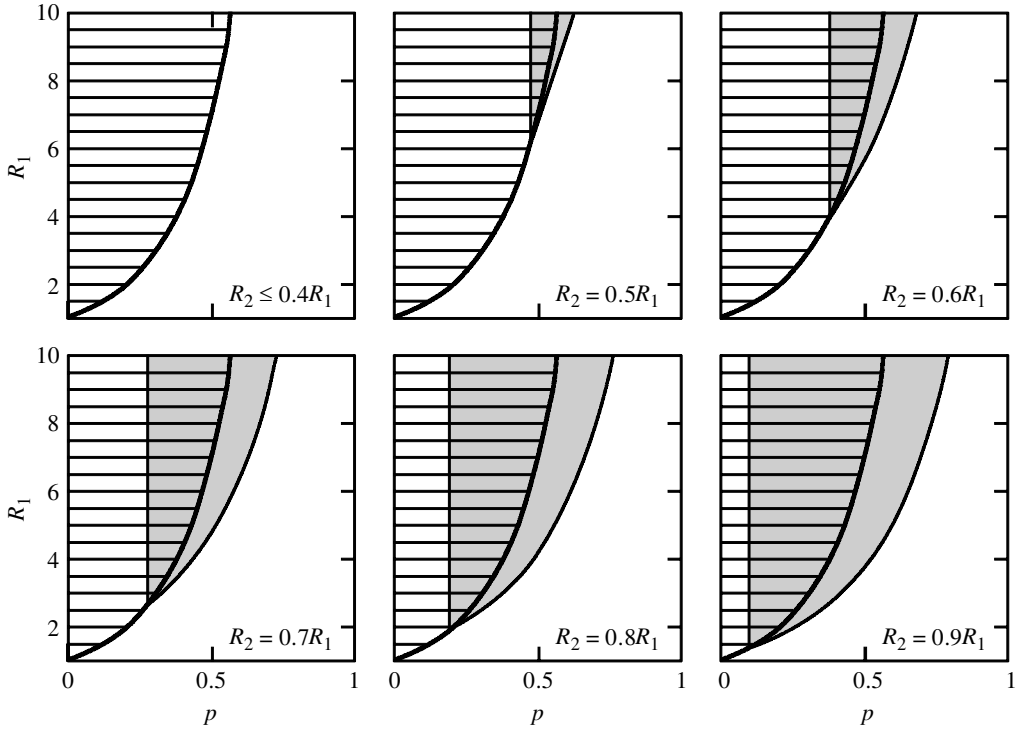

Figure 4. Therapy outcome as a function of adherence for a single drug regimen. Therapy outcome is illustrated as a function of adherence, (p, x-axis), the basic reproductive ratio of the drug-sensitive virus (R_1, y-axis) and the ratio of R_1 to R_2 (panels). The solid black line in each panel shows the degree of adherence at which $R_1 = 1$. In regions to the left of this line, treatment will fail to eliminate the drug-sensitive virus (horizontal hatching). The grey region in each figure shows parameter values for which the resistant mutant will dominate the system, either by out-competing the drug-sensitive virus (to the left of the solid line, $R_2 > R_1 > 1$), or by surviving in a situation where the wild-type virus cannot survive (to the right of the line, $R_2 > 1 > R_1$). Thus regions to the right of the solid line show parameter values for which the emergence of resistant virus will cause treatment failure, for a drug regimen and adherence that would be sufficient to eliminate the wild-type alone. We use parameters which approximate the effect of the protease inhibitor ritonavir ($T_{1/2} = 4$ h, $T = 12$ h and $C_{max} = 11.2\,\mu g\,ml^{-1}$). For the drug-sensitive strain we set $IC_{50} = 0.0159\,\mu g\,ml^{-1}$, while IC_{50} for the drug-resistant strain is ten times greater ($0.159\,\mu g\,ml^{-1}$).

grey shading, either by out-competing the drug-sensitive virus (grey shading to the left of the black line) or by surviving in a situation where the drug-sensitive virus would be eliminated (grey shading to the right of the black line).

For this example we model the effect of the protease inhibitor ritonavir,which is typically taken every 12 h and has a 4 h half-life, and once again return to the Poisson pattern of adherence. Phenotypic and genotypic testing of HIV isolates from patients treated with ritonavir have shown a number of mutations in the virus protease gene which confer a 2.5-fold to eightfold resistance to the drug *in vitro* (for reviews, see Lea & Faulds 1996; Moyle & Gazzard 1996; Hoetelmans *et al.* 1997; McDonald & Kuritzkes 1997).

Figure 4 illustrates a few key points. Note, first, that when the basic reproductive ratio of the drug-resistant virus is much smaller than the wild-type R_0, there is no region where resistance can emerge ($R_2 \leqslant 0.4R_1$). In this case, increasing adherence moves directly from regions of failure (failure to eliminate y_1) to treatment success. Likewise, if the basic reproductive ratio of the wild-type virus is small (less than two or three), treatment is successful for very low levels of adherence (anything over $p \approx 0.4$), and if treatment fails it is probably due to the persistence of the drug-sensitive virus: resistance is very unlikely to emerge. The critical feature of the system, however, appears to be the ratio of the pre-treatment R_2 to the pre-treatment R_1. If this ratio is higher than about 0.7, and if R_1 is higher than 2 or 3, resistance is very likely to dominate the system after treatment. For many cases even 80% adherence with this single drug will not be sufficient to eliminate the drug-resistant virus.

(b) *Combination therapy*

We repeated this analysis for triple-drug therapy, using the standard regimen of two nucleoside analogue reverse transcriptase inhibitors (3TC and AZT) and a single protease inhibitor (ritonavir). Phenotypic studies have shown HIV isolates with over 500-fold resistance to 3TC; this resistance emerges rapidly, in weeks to months (Schuurman *et al.* 1995; Mayers 1996). For AZT, mutations typically emerge over months or years and may confer up to 100-fold resistance (Richman *et al.* 1994; de Jong *et al.* 1996; Mayers 1996). For the results presented below, we assumed that the viral strains resistant to 3TC have a 200-fold resistance, those strains resistant to AZT have a 100-fold resistance, and those resistant to ritonavir have a tenfold resistance.

We define the dosing interval and time-course separately for each drug, modelling the fraction of doses taken independently for each one, but combining the effects of all three drugs as described above when computing R_1. We then compute R_i at each time for a number of possible drug-resistant strains, y_i. In this example we consider a total of seven drug-resistant strains: three that are only

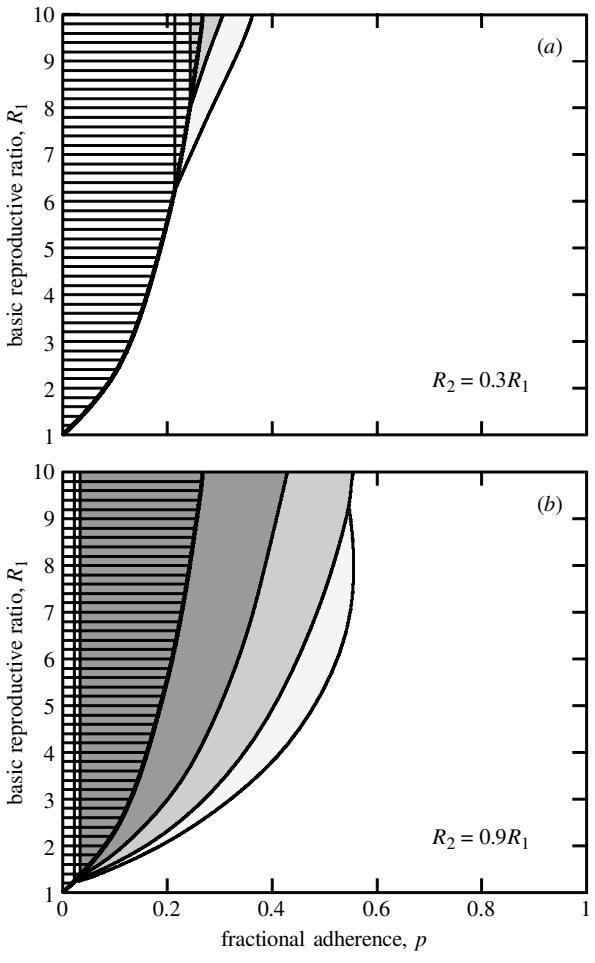

Figure 5. Therapy outcome as a function of adherence for triple-drug regimen.Therapy outcome is illustrated as a function of adherence (p, x-axis), and the basic reproductive ratio of the drug-sensitive virus (R_1, y-axis). Here the ratio of R_2 to R_1 is 0.3 (*a*) or 0.9 (*b*). The solid black line shows the degree of adherence at which $R_1 = 1$. Therapy outcome is as described in the text: in brief, grey regions illustrate regions of treatment failure due to the emergence of viral strains resistant to one, two or three of the drugs. We find that treatment fails at higher degrees of adherence for multiply resistant viral strains, if these strains exist. We also note that triple-drug therapy is robust to higher levels of non-adherence than single-drug therapy. For this example we used a drug regimen which approximates the combination of 3TC, AZT and ritonavir (drug 1: $T_{1/2} = 6$ h, $\mathcal{T} = 12$ h, $C_{max} = 5\,\mu$M, IC_{50}(sensitive) $= 0.0197\,\mu$M, IC_{50}(resistant) $= 3.94\,\mu$M; drug 2: $T_{1/2} = 1$ h, $\mathcal{T} = 12$ h, $C_{max} = 5.5\,\mu$M, IC_{50}(sensitive) $= 0.0234\,\mu$M, IC_{50}(resistant) $= 2.34\,\mu$M; drug 3: $T_{1/2} = 4$ h, $\mathcal{T} = 12$ h, $C_{max} = 11.2\,\mu g\,ml^{-1}$, IC_{50}(sensitive) $= 0.0159\,\mu g\,ml^{-1}$, IC_{50}(resistant) $= 0.159\,\mu g\,ml^{-1}$).

resistant to one of the three drugs, three that are resistant to two of the three drugs, and one that is resistant to all three drugs in the cocktail. For simplicity we have assumed that all the drug-resistant strains have the same infectivity (β_2), which is less than the infectivity of the wild-type. We have neglected cross-resistance (resistance to one drug does not confer any advantage when facing the other drugs), and have also ignored possible drug–drug interactions, which may alter the concentration time-course when antivirals are taken in combination.

The results of this analysis appear in figure 5, for two different ratios of wild-type and resistant infectivities. As in figure 4, the region to the left of the thick black line (horizontal hatching in both panels) corresponds to treatment failure—the wild-type virus is not eliminated by the drug, regardless of whether resistant virus stains are present. The white region on the right of both panels corresponds to treatment success. Considering figure 5*b* first, for the case when the drug-resistant mutants are only slightly less infective than the wild-type, the central regions can be described as follows.

Suppose that resistant mutants exist which are resistant to one of the three drugs, but no resistant strains that are resistant to several drugs exist. Resistance will then arise in the large dark grey region in the centre of the plot. To the left of that region treatment fails by failing to eliminate y_1, while to the right of that region treatment succeeds.

If, however, mutants exist which are resistant to one or two drugs, resistance will arise over a larger area. Anywhere within the middle grey region or dark grey central region of the graph, a mutant which is resistant to two of the three drugs will dominate. Finally, if mutants exist which are resistant to all three drugs, they will dominate anywhere within the light grey, middle grey or dark grey central regions.

In figure 3*a* we see that if the pre-treatment cost of resistance is sufficiently high, treatment is likely either to fail (to eliminate the wild-type virus) or to succeed; parameter values for which resistant mutants are predicted to arise and dominate the system are rare. We note, however, that once resistance has emerged during therapy the viral load does not necessarily reflect this pre-treatment cost of resistance (see § 5).

We see from these results that viral strains with multiple resistance are able to dominate the system for higher degrees of adherence—but of course these strains are less likely to exist. We also note the increased efficacy of triple-drug over single-drug therapy. Treatment is successful over a wider range of adherence levels and resistance of any sort, on the whole, is less likely to emerge. We conclude that triple-drug therapy is more robust to non-adherence than single-drug therapy. Finally, we note that in this example, treatment is most likely to fail by the emergence of a viral strain that is resistant to one of the three drugs.

5. DISCUSSION

In this system, the basic reproductive ratio rises and falls with drug concentration, as shown in figure 1. This variation occurs over hours, whereas the time-scale of therapy outcome is months or years. Our model predicts that the relevant predictor of therapy outcome is the long-term average of R_0, which is proportional to the long-term average of the antiviral effect s. This result is in contrast to the intuitive notion that a qualitative change might occur if R_0 becomes briefly greater than unity when, for example, a dose of the drug is missed. Although each missed dose does have a detrimental effect on the long-term antiviral effect (altering $\bar{s}$ significantly), we find that the long-term pattern of adherence is more important than whether the virus has been allowed to replicate effectively for short intervals. This suggests the possibility of analysing clinical data by aggregating individuals depending on long-term averages of adherence, despite considerable variation in

dose-taking patterns. We emphasize, however, that the long-term antiviral effect may differ for different dose-taking patterns, even though the total adherence (total fraction of doses taken) is the same.

Our conclusions do not consider the possibility that the virus population may evolve towards synchronization with the pattern of drug therapy. If the life cycle of the virus is a multiple of the dosing interval, it is possible that over time the bulk of the virus population will replicate during trough concentrations of the drug, when R_0 is highest. This suggests a possibility for future work.

Our model predicts that non-adherence allows resistant strains (which already exist at very low frequencies in the pre-treatment host; Ribeiro *et al.* 1998) to grow exponentially, dominating the system after some months. The time taken for the resistant mutant to emerge can be very long if the basic reproductive ratios of the sensitive and resistant viral strains are close. Although it is unlikely that successful drug therapy will allow new resistant strains to emerge during treatment (Bonhoeffer *et al.* 1997*b*), the degree to which this holds for imperfect drug therapy is unclear. Non-adherence may play a key role in the 'fine-tuning' of resistance over time. Thus, another direction for future study is the effect of adherence on the evolution of gradually more resistant and multiply resistant strains of the virus.

Finally, as discussed more fully in Bonhoeffer & Nowak (1997), this basic model of viral dynamics is only able to explain a ten- to 100-fold reduction in virus load during therapy if the basic reproductive ratio of the virus during therapy is very close to unity. While this assumption appears unrealistic, we point out that increasing adherence reduces R_0 for both the resistant and sensitive virus (figure 3). Resistance is only able to emerge when the basic reproductive ratio of the drug-sensitive virus falls below unity, while R_0 for the drug-resistant virus is still greater than unity. If the (pre-treatment) infectivities of these two strains are close, it becomes plausible that R_0 for the drug-resistant virus is close to unity when this occurs. The inclusion of an immune response in the model may also reduce this problem, and may dampen the oscillatory dynamics described by McLean & Nowak (1992).

We gratefully acknowledge the support of the Leon Levy and Shelby White Initiatives Fund, the Florence Gould Foundation, the Ambrose Monell Foundation, the Seaver Institute, and the Alfred P. Sloan Foundation.

APPENDIX A. MEAN VALUE OF THE INHIBITORY EFFECT, $\bar{s}(p)$

For perfect adherence, $\bar{s}$ is just the area under $s(t)$ for one dosing interval, divided by the length of the interval T. We find that

$$\begin{aligned}\bar{s}(p) &= \frac{1}{T}\int_0^T s(t)\,\mathrm{d}t \\ &= \frac{1}{T}\int_0^T \left(1 - \frac{C_{\max}\mathrm{e}^{-wt}}{C_{\max}\mathrm{e}^{-wt} + \mathrm{IC}_{50}}\right)\mathrm{d}t \\ &= 1 + \frac{1}{Tw}\left(\log\left(C_{\max}\mathrm{e}^{-wT} + \mathrm{IC}_{50}\right) - \log\left(C_{\max} + \mathrm{IC}_{50}\right)\right).\end{aligned} \tag{A1}$$

In solving this equation we have set t_p in equation (1) to be zero, i.e. we assume that the drug concentration peaks instantaneously when the dose is taken.

More generally, we can compute $\bar{s}$ as a weighted average of the areas under $s(t)$ after a dose is taken, after a single dose is missed, after two successive doses are missed, etc. If we let A_i be the area under $s(t)$ for a dosing interval that occurs immediately after i doses have been missed in succession, we find that

$$\begin{aligned}A_i &= \int_{t=iT}^{(i+1)T}\left(1 - \frac{C_{\max}\mathrm{e}^{-wt}}{C_{\max}\mathrm{e}^{-wt} + \mathrm{IC}_{50}}\right)\mathrm{d}t \\ &= T + \frac{1}{w}\left(\log\left(C_{\max}\mathrm{e}^{-(i+1)wT} + \mathrm{IC}_{50}\right)\right. \\ &\quad \left. - \log\left(C_{\max}\mathrm{e}^{-iwT} + \mathrm{IC}_{50}\right)\right).\end{aligned} \tag{A2}$$

For the Poisson model of adherence described in the text, it is clear that $P_i(p)$, the probability that i successive doses were missed after the last dose was taken, is given by $p(1-p)^i$. Thus for this adherence pattern we can compute

$$\bar{s}(p) = \frac{1}{T}\sum_{i=0}^{\infty} P_i(p)A_i. \tag{A3}$$

In writing this equation we assume that no matter how small p is, a single dose was taken at time zero. (When $p = 0$, we set $\bar{s} = 1$.) We can use this equation to approximate $\bar{s}_1(p)$ and $\bar{s}_2(p)$ by using the appropriate values for drug-sensitive and drug-resistant IC_{50}.

For the blocked model of adherence described in the text (and block-size n), we let $P_i(p)$ be the probability that i successive blocks were missed after the last block of doses was taken, and simply define a block of doses taken as n successive doses, or a block of doses missed as n successive missed doses. In this case we find that $P_i(p) = p(1-p)^i$ as before, but now we define B_i as the area under $s(t)$ for a dosing block that occurs immediately after i blocks have been missed in succession.

It is clear that $B_0 = A_0$, and for higher values of i we find

$$B_i = \frac{1}{n}\sum_{j=n(i-1)+1}^{j=ni} A_j. \tag{A4}$$

REFERENCES

Anderson, R. M. & May, R. M. 1991 *Infectious diseases of humans: dynamics and control.* Oxford University Press.

Austin, D. J. & Anderson, R. M. 1999 Studies of antibiotic resistance within the patient, hospitals and the community using simple mathematical models. *Phil. Trans. R. Soc. Lond.* B **354**, 721–738.

Austin, D. J., Kakehashi, M. & Anderson, R. M. 1997 The transmission dynamics of antibiotic-resistant bacteria: the relationship between resistance in commensal organisms and antibiotic consumption. *Proc. R. Soc. Lond.* B **264**, 1629–1638.

Austin, D. J., White, N. J. & Anderson, R. M. 1998 The dynamics of drug action on the within-host population growth of infectious agents: melding pharmacokinetics with pathogen population dynamics. *J. Theor. Biol.* **194**, 313–339.

Austin, D. J., Kristinsson, K. G. & Anderson, R. M. 1999 The relationship between the volume of antimicrobial consumption in human communities and the frequency of resistance. *Proc. Natl Acad. Sci. USA* **96**, 1152–1156.

Besch, C. L. 1995 Compliance in clinical trials. *AIDS* **9**, 1–10.
Bonhoeffer, S. & Nowak, M. A. 1997 Pre-existence and emergence of drug resistance in HIV-1 infection. *Proc. R. Soc. Lond.* B **264**, 631–637.
Bonhoeffer, S., Lipsitch, M. & Levin, B. R. 1997*a* Evaluating treatment protocols to prevent antibiotic resistance. *Proc. Natl Acad. Sci. USA* **94**, 12 106–12 111.
Bonhoeffer, S., May, R. M., Shaw, G. M. & Nowak, M. A. 1997*b* Virus dynamics and drug therapy. *Proc. Natl Acad. Sci. USA* **94**, 6971–6976.
Coffin, J. M. 1995 HIV population dynamics in vivo: implications for genetic variation, pathogenesis and therapy. *Science* **267**, 483–489.
Davies, J. E. 1997 Origins, acquisition and dissemination of antibiotic resistance determinants. *Ciba Found. Symp.* **207**, 15–27.
de Jong, M. D., Veenstra, J., Stilianakis, N. I., Schuurman, R., Lange, J. M., de Boer, R. J. & Boucher, C. A. 1996 Host–parasite dynamics and outgrowth of virus containing a single K70R amino acid change in reverse transcriptase are responsible for the loss of human immunodeficiency virus type 1 RNA load suppression by zidovudine. *Proc. Natl Acad. Sci. USA* **93**, 5501–5506.
Dietz, K. 1975 Transmission and control of arbovirus diseases. In *Epidemiology* (ed. D. Ludwig & K. L. Cooke), pp. 104–121. Philadelphia, PA: SIAM.
Dietz, K. 1976 The incidence of infectious diseases under the influence of seasonal fluctuations. *Lect. Notes Biomath.* **11**, 1–15.
Frost, S. D. W. & McLean, A. R. 1994 Quasispecies dynamics and the emergence of drug resistance during zidovudine therapy of HIV infection. *AIDS* **8**, 323–332.
Hoetelmans, R. M., Meenhorst, P. L., Mulder, J. W., Burger, D. M., Koks, C. H. & Beijnen, J. H. 1997 Clinical pharmacology of HIV protease inhibitors: focus on saquinavir, indinavir, and ritonavir. *Pharmacol. World Sci.* **19**, 159–175.
Ickovics, J. R. & Meisler, A. W. 1997 Adherence in AIDS clinical trials: a framework for clinical research and clinical care. *J. Clin. Epidemiol.* **50**, 385–391.
Jarvis, B. & Faulds, D. 1998 Nelfinavir. A review of its therapeutic efficacy in HIV infection. *Drugs* **56**, 147–167.
Katzenstein, D. A. 1997 Adherence as a particular issue with protease inhibitors. *J. Assoc. Nurses AIDS Care* **8** (Suppl.), 10–17.
Kepler, T. B. & Perelson, A. S. 1998 Drug concentration heterogeneity facilitates the evolution of drug resistance. *Proc. Natl Acad. Sci. USA* **95**, 11 514–11 519.
Lea, A. P. & Faulds, D. 1996 Ritonavir. *Drugs* **52**, 541–546.
Levin, S. A. & Andreason, V. 1999 Disease transmission dynamics and the evolution of antibiotic resistance in hospitals and communal settings. *Proc. Natl Acad. Sci. USA* **96**, 800–801.
Levin, B. R., Lipsitch, M., Perrot, V., Schrag, S., Antia, R., Simonsen, L., Walker, N. M. & Stewart, F. M. 1997 The population genetics of antibiotic resistance. *Clin. Infect. Dis.* **24** (Suppl. 1), S9–S16.
Levin, B. R. (and 19 others) 1998 Resistance to antimicrobial chemotherapy: a prescription for research and action. *Am. J. Med. Sci.* **315**, 87–94.
Levin, S. A., Lipsitch, M. & Bonhoeffer, S. 1999 Population biology, evolution, and infectious disease: convergence and synthesis. *Science* **283**, 806–809.
Levy, S. B. 1997 Antibiotic resistance: an ecological imbalance. *Ciba Found. Symp.* **207**, 1–9.
Lipsitch, M. & Levin, B. R. 1997 The population dynamics of antimicrobial chemotherapy. *Antimicrob. Agents Chemother.* **41**, 363–373.
Lipsitch, M. & Levin, B. R. 1998 The population dynamics of tuberculosis chemotherapy: mathematical models of the roles of noncompliance and bacterial heterogeneity in the evolution of drug resistance. *Int. J. Tuberculosis Lung Dis.* **2**, 187–199.
Macdonald, G. 1952 The analysis of equilibrium in malaria. *Trop. Dis. Bull.* **49**, 813–829.
McDonald, C. K. & Kuritzkes, D. R. 1997 Human immunodeficiency virus type 1 protease inhibitors. *Arch. Intern. Med.* **157**, 951–959.
McLean, A. R. & Nowak, M. A. 1992 Competition between zidovudine-sensitive and zidovudine-resistant strains of HIV. *AIDS* **6**, 71–79.
May, R. M. & Anderson, R. M. 1979 Population biology of infectious diseases II. *Nature* **280**, 455.
Mayers, D. 1996 Rational approaches to resistance: nucleoside analogues. *AIDS* **10** (Suppl. 1), S9–S13.
Mehta, S., Moore, R. D. & Graham, N. M. 1997 Potential factors affecting adherence with HIV therapy. *AIDS* **11**, 1665–1670.
Moyle, G. & Gazzard, B. 1996 Current knowledge and future prospects for the use of HIV protease inhibitors. *Drugs* **51**, 701–712.
Nowak, M. A., Anderson, R. M., McLean, A. R., Wolfs, T. F. W., Goudsmit, J. & May, R. M. 1991 Antigenic diversity thresholds and the development of AIDS. *Science* **254**, 963–969.
Nowak, M. A., Bonhoeffer, S., Shaw, G. M. & May, R. M. 1997 Anti-viral drug treatment: dynamics of resistance in free virus and infected cell populations. *J. Theor. Biol.* **184**, 203–217.
Paterson, D., Swindells, S., Mohr, J., Brester, M., Vergis, E., Squier, C., Wagener, M. & Singh, N. 1999 How much adherence is enough? A prospective study of adherence to protease inhibitor therapy using MEMSCaps. In *Proceedings of the Sixth Conference on Retroviruses and Opportunistic Infections, Chicago, IL*, Abstract 092.
Ribeiro, R. M., Bonhoeffer, S. & Nowak, M. A. 1998 The frequency of resistant mutant virus before anti-viral therapy. *AIDS* **12**, 461–465.
Richman, D. D., Meng, T. C., Spector, S. A., Fischl, M. A., Resnick, L. & Lai, S. 1994 Resistance to AZT and ddC during long-term combination therapy in patients with advanced infection with human immunodeficiency virus. *J. AIDS* **7**, 135–138.
Schuurman, R. (and 12 others) 1995 Rapid changes in human immunodeficiency virus type 1 RNA load and appearance of drug-resistant virus populations in persons treated with lamivudine (3TC). *J. Infect. Dis.* **171**, 1411–1419.
Stilianakis, N. I., Boucher, C. A., de Jong, M. D., Van Leeuwen, R., Schuurman, R. & de Boer, R. J. 1997 Clinical data sets of human immunodeficiency virus type 1 reverse transcriptase-resistant mutants explained by a mathematical model. *J. Virol.* **71**, 161–168.
United States Department of Health and Human Services 1999 Adherence to potent antiretroviral therapy. In *Guidelines on the optimal use of antiretroviral therapies in HIV infected adults and adolescents*. Available at http://www.aids.wustl.edu/aids/clinguide.html.
Yorke, J. A., Nathanson, N., Pianingiani, G. & Martin, J. 1979 Seasonality and the requirements for perpetuation and eradication of viruses. *Am. J. Epidemiol.* **109**, 103–123.

As this paper exceeds the maximum length normally permitted, the authors have agreed to contribute to production costs.